Multi-pulse enhanced laser ion acceleration using plasma half cavity targets

G. G. Scott, J. S. Green, V. Bagnoud, C. Brabetz, C. M. Brenner, D. C. Carroll, D. A. MacLellan, A. P. L. Robinson, M. Roth, C. Spindloe, F. Wagner, B. Zielbauer, P. McKenna, and D. Neely

Citation: Applied Physics Letters **101**, 024101 (2012); doi: 10.1063/1.4734397
View online: http://dx.doi.org/10.1063/1.4734397
View Table of Contents: http://scitation.aip.org/content/aip/journal/apl/101/2?ver=pdfcov
Published by the AIP Publishing

Multi-pulse enhanced laser ion acceleration using plasma half cavity targets

G. G. Scott,[1,2] J. S. Green,[1] V. Bagnoud,[3] C. Brabetz,[3] C. M. Brenner,[1,2] D. C. Carroll,[2] D. A. MacLellan,[2] A. P. L. Robinson,[1] M. Roth,[4] C. Spindloe,[1] F. Wagner,[3,4] B. Zielbauer,[3] P. McKenna,[2] and D. Neely[1,2]
[1]*Central Laser Facility, STFC Rutherford Appleton Laboratory, OX11 0QX Didcot, United Kingdom*
[2]*Department of Physics SUPA, University of Strathclyde, G4 0NG Glasgow, United Kingdom*
[3]*PHELIX Group, Gesellschaft für Schwerionenforschung, D-64291 Darmstadt, Germany*
[4]*Fachbereich Physik, Technische Universität Darmstadt, D-64289 Darmstadt, Germany*

(Received 17 April 2012; accepted 20 June 2012; published online 10 July 2012)

We report on a plasma half cavity target design for laser driven ion acceleration that enhances the laser to proton energy conversion efficiency and has been found to modify the low energy region of the proton spectrum. The target design utilizes the high fraction of laser energy reflected from an ionized surface and refocuses it such that a double pulse interaction is attained. We report on numerical simulations and experimental results demonstrating that conversion efficiencies can be doubled, compared to planar foil interactions, when the secondary pulse is delivered within picoseconds of the primary pulse. © *2012 American Institute of Physics*.
[http://dx.doi.org/10.1063/1.4734397]

The field of laser plasma interactions has become an area of growing interest, with the advance of laser parameters over the past two decades paving the way toward applications. In the ultraintense regime ($10^{18} - 10^{21}$ Wcm^{-2}) available at many high power laser facilities, ions can be accelerated from the rear surface of typically micron thick targets via the process of target normal sheath acceleration (TNSA).[1] Laser driven ion acceleration is particularly interesting due to the potential applications, including medical treatments[2] and (isochoric) heating of matter,[3] which has been proposed by many as an attractive method for heating nuclear fuel in fusion reactions. In theory, the quasi thermal TNSA spectrum works well for this,[4] with ignition predicted to be possible with currently achievable proton temperatures of $\sim$3 MeV. However, conversion efficiencies of laser energy to protons must be increased beyond the few percent so far routinely reported in the literature to upward of 10% for this to be a feasible concept.[5]

In many laser plasma interactions in the region of 60% of the total incident laser energy has been measured to be reflected from the target;[6] a fraction found to be almost intensity independent over four orders of magnitude[7] up to 10^{21} Wcm^{-2}. In this paper, a target design is introduced (Fig. 1(a)) which is engineered to reuse the large fraction of laser energy reflected from the initial interaction to increase conversion efficiency of the laser energy into protons. In this scheme, in addition to the planar (accelerating) foil that the laser primarily interacts with, a second (cavity) foil forms a half cavity which collects the reflected laser light and returns it back towards the initial interaction point. In addition to being returned, the laser light is refocused by shaping the cavity foil in the form of a quarter sphere, maintaining a high beam intensity. Non cavity focusing plasma optics have been examined by Nakatsutsumi *et al.*[8] and non focusing cavities are also beginning to be explored by Badziak *et al.*[9]

The scheme reported here gives rise to a double pulse interaction with the accelerating foil (Fig. 1(b)). The intensity ratio of the initial pulse to the post pulse is determined by the combined reflected energy fraction, F, from the surface of the accelerating foil and the interior surface of the cavity foil. The delay between the pulses, $\delta\tau$, is simply determined by the time taken for the laser light to travel twice the radius, r, of the half cavity. By altering the half cavity radius, the timing of the delivery of the post pulse can be varied and chosen to optimize laser energy coupling to ions.

The use of multiple pulses to enhance and control the ion acceleration process has been investigated via simulation[10] and experimentally.[11] By irradiating planar foils with a controlled prepulse followed by a 2×10^{19} Wcm^{-2} main pulse, an increased conversion efficiency of laser energy to protons by a factor of 3.3 was demonstrated using a prepulse containing 10% of the total incident energy.[11] The present scheme differs from previous work in that the main pulse is followed by a post pulse containing $\sim$ 40% of the main pulse energy.

An experimental campaign was carried out using the Petawatt High Energy Laser for heavy Ion eXperiments (PHELIX) at the Gesellschaft für Schwerionenforschung (GSI) facility, where the s-polarised laser is delivered in 0.5 ps pulses with typical energies of 105 J on target. The beam is focused using an *f*/9 off axis parabola (at a 39° angle of incidence) to a 20×15 μm FWHM elliptical spot giving on target intensities of $\sim 10^{19}$ Wcm^{-2}. The pulse has a nanosecond contrast ratio of 10^6, where contrast is defined as the intensity ratio of the main pulse to the amplified spontaneous emission prepulse of the laser system. The primary diagnostic for proton dosimetry was radiochromic film (RCF), which was used in a stack configuration to enable proton doses to be measured in discrete energy steps as well as providing the two dimensional spatial intensity distribution of the beam at selected energies. With shock velocities of several microns per nanosecond being induced by nanosecond prepulses,[12] a 25 μm thick gold accelerating foil was selected to ensure that any shocks would not break out from the back of the target during the ion acceleration process.

As the Rayleigh length of the focusing optic is approximately 100 μm, the beam intensity on the cavity interior

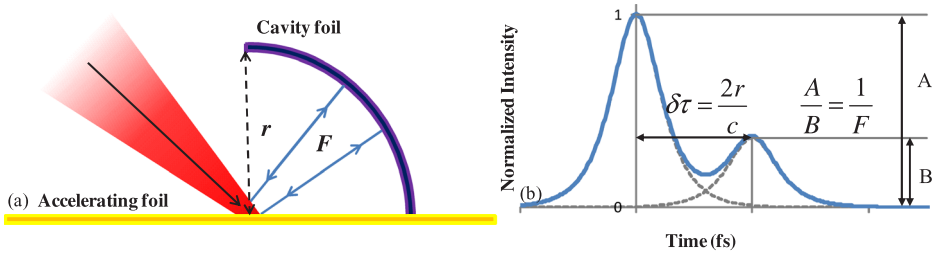

FIG. 1. (a) Schematic diagram showing the incoming main pulse being reflected by a target foil. A plasma half cavity is used to back reflect and refocus the laser energy onto the target. (b) The intensity ratio of the pulses is determined by the combined reflected energy fraction, F, of the accelerating foil front surface and cavity foil interior, the delay between the pulses, $\delta\tau$, is set as $2r/c$ where r is the radius of the half cavity.

remains $\sim 10^{17} - 10^{18}$ Wcm^{-2} and is sufficient to generate a secondary TNSA proton beam at 39° to the forward direction. With lower laser intensity on the cavity foil a smaller number of protons with a lower temperature and maximum energy are expected from this interaction compared to those from the accelerating foil,[13] with a larger divergence due to the curvature of the target. The majority of these protons with energies below ~ 3.4 MeV are stopped in the accelerating foil. The combination of these effects make it unlikely that secondary protons will make a significant contribution to the measured dose or be detectable for larger cavities where intensities on the cavity interior are lower. However, to avoid the detection of any higher energy secondary protons the RCF detector stack is positioned at a distance of 37 mm from the target such that any secondary beam would be well separated from the main beam in the detector plane.

The proton energy spectra obtained for four shots in the experimental campaign are presented in Fig. 2(a). These were obtained for constant laser parameters incident on a single planar foil target as a control measurement and three plasma half cavity targets with radii of 100 μm, 210 μm, and 260 μm, corresponding to $\delta\tau$ of 670 fs, 1400 fs, and 1730 fs, respectively. The interaction of the laser pulse with the planar foil is found to give the single temperature quasi Maxwellian proton spectra typically observed in laser plasma interactions in this intensity regime. On introduction of the two larger half cavity targets a significant increase in laser to proton energy conversion efficiency of $\sim 55\%$ is observed in the lower half of the energy spectrum and generally a higher proton number is measured over the full energy spectrum for all half cavities. This is shown more clearly by plotting the enhancement factors (Fig. 2(b)), where the dose observed at a given proton energy is normalized to the dose obtained at the same energy for the planar foil interaction. In general, the enhancement factor is larger at higher proton energies suggesting a slight increase in proton temperature which may be explained by an effective pulse duration increase seeding hot electrons in the sheath for a longer time; similarly, this may increase the maximum proton energy.[13–15] However, no target geometry showed dose above signal to noise on the RCF layer corresponding to proton energy of 15.2 MeV, with all having detectable dose at 13.8 MeV on the previous layer. With proton numbers exponentially decreasing as energy increases it is clear that the total conversion efficiency enhancement is dominated by the number of protons accelerated in the low energy region of the spectrum.

The interactions involving the smallest radius half cavity show smaller but generally similar enhancement trends across the spectrum but with a pronounced dose enhancement at 3.2 MeV, where three and a half times the number of protons are produced compared to the planar foil interaction. This may be explained by a peak in the proton spectra, which is predicted in simulation of multi-pulse interactions,[10] and the finite width of the RCF active layer indicates that any spectral peak would lie in the range of 3.2–3.3 MeV. The 2D spatial intensity distribution and divergence of the protons are very similar for both the planar foil and cavity target shots, strongly indicating that the protons come from a single source and that the mechanism responsible for the enhancement and the spectral feature originates in the sheath of the accelerating foil.

The energy spectra in Figure 2(a) were treated and numerically integrated using the composite trapezoidal rule. These integrals were normalized to that obtained for the planar foil, giving a normalized conversion efficiency, shown in Figure 3. Here, the total proton conversion efficiency is observed to be doubled for the 100 μm radius half cavity, and a $\sim 55\%$ enhancement is observed for the larger half cavity radii tested. The experimental data is compared with simulations using the one dimensional particle in cell (PIC) code, ELPS.[10]

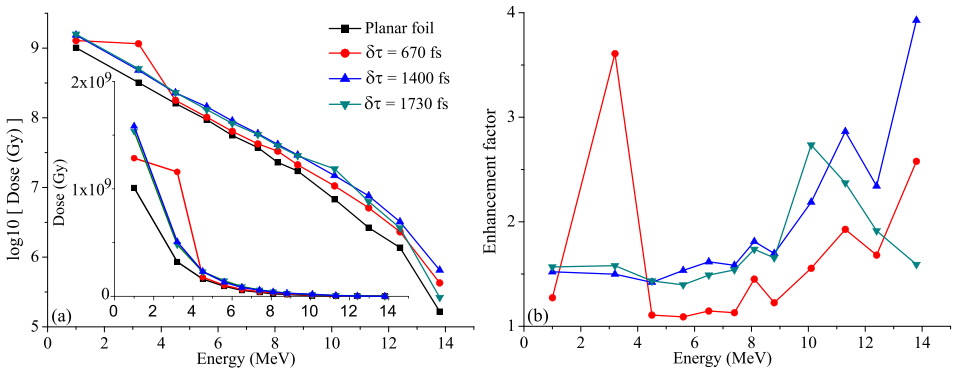

FIG. 2. (a) The proton spectra for a planar foil and three of the half cavity target geometry tested, inset: linear scale. (b) The enhancement factor (defined in text) as a function of energy for each of the plasma half cavity proton spectra.

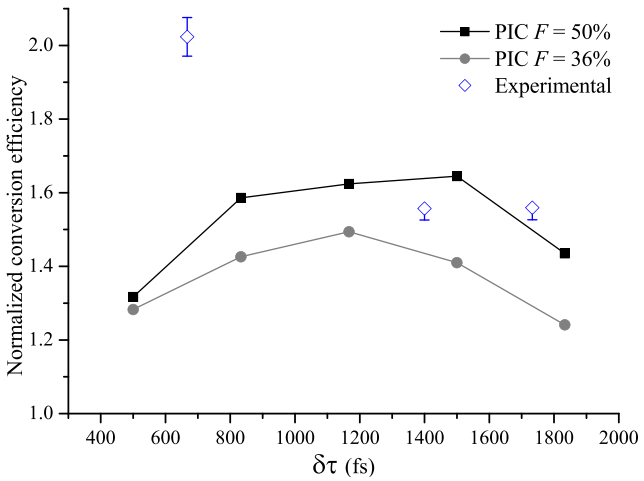

FIG. 3. The integrated experimental doses compared with simulation results. Both experimental and simulation results are normalized to the corresponding single pulse planar foil interactions.

In the simulations a main pulse was followed by a post pulse of variable intensity ratio determined by F and with $\delta\tau$ ranging from 0.5 ps to 1.8 ps corresponding to a half cavity radius range of 75 μm to 275 μm. Simulations had 2.5×10^5 electron, proton, and ion macroparticles each, with each species initially uniformly distributed through a one micron region of the grid representing the target. By using a reduced target thickness realistic target densities were achieved while keeping the number of macroparticles low enough for feasible simulation times. Simulations were run in a box of sufficient width to contain the whole interaction over the 4 ps simulation duration, where the simulation duration was chosen to allow sufficient time for protons to approach their final energy asymptote. Foil ions were given sufficient mass to remain static throughout the interaction and were assigned a charge state of one, again to keep electron numbers low. A laser of wavelength 1.053 μm and 0.5 ps duration was used, with intensities defined through the dimensionless laser parameter, a_0, equal to 4.1 for the main pulse reflecting typical experimental parameters. A reference simulation was run representing a single laser pulse ($a_0 = 4.1$) interacting with a planar foil.

A second reference simulation was run to investigate the energy scaling of the single pulse interaction. This was done to separate the effect of the enhanced laser energy from the dual pulse effect, both of which occur due to the energy reflected from the cavity. Here, the sum of the energy of the primary and secondary pulses was contained within a single 0.5 ps pulse and therefore $a_0 = 4.8$, due to the additional 36% energy.

The total proton conversion efficiency for simulations involving double pulse interactions are normalized to the total proton conversion efficiency given by a single pulse interaction ($a_0 = 4.1$), and these are presented in Figure 3. F values of, 0.36 and 0.50 were simulated and it was found that for $F = 0.36$, the proton yield is increased on introduction of a post pulse, and is predicted to be optimized for a delay of ~ 1.2 ps, with an enhancement of 50% compared to the planar foil shot. As F increases further to 0.50 the conversion efficiency can be improved by as much as 65%.

Both simulation and experimental results show a correlation between $\delta\tau$ and the proton conversion efficiency. The time delay between pulses is important both from the laser plasma interaction perspective and also in terms of the multi-pulse effects at the rear of the target. An increase in the scale length of underdense plasma on the front surface has been shown to enhance proton acceleration and increase the maximum proton energy;[16] this is attributed to self focusing and absorption of the laser beam in the preplasma.[17] In the half cavity target geometry the primary pulse interaction with the foil seeds plasma expansion on the front surface which the secondary pulse goes on to interact with and as the delay between the two pulses increases the scale length that the secondary pulse interacts with also increases, potentially giving enhanced laser energy to proton conversion efficiency. Similarly, there is a plasma expansion on the target rear through TNSA and as the secondary pulse arrives later in time the hot electrons are injected into a longer scale length expanding plasma, which has been shown to cause inferior electric fields to be generated than in the sharp boundary case.[18,19] This results in an optimum delay where the two effects are balanced.

The reference simulations also show that when an $a_0 = 4.8$ single 0.5 ps pulse is used, an increase in proton conversion efficiency of $\sim 20\%$ is observed. Therefore by using a half cavity target to stage the delivery of the energy to the system a greater enhancement is achieved than by a single pulse with the same total energy.

In simulations, the primary pulse interacts with an initially infinitely steep density gradient on the front of the target. However, prepulses in the real laser system are sufficient to cause a plasma expansion on the nanosecond time scale, this may cause a shift in the critical surface position which would in turn lead to a shift in the optimum plasma half cavity radius observed experimentally.

The experimentally found enhancement in the laser to proton energy conversion efficiency for larger $\delta\tau$ is consistent with simulations for F in the region of 0.36 to 0.50 yielding a $\sim 50\%$ enhancement in the conversion efficiency. However, there is a clear discrepancy between the enhancement expected for small $\delta\tau$ and that measured experimentally, predominantly due to the high dose low energy feature not predicted by the PIC code. Half cavities with $\delta\tau$ of 1400 fs or larger give a temporal intensity profile on the accelerating foil where the main pulse and post pulse can be considered to be temporally separate. However, the smaller radii half cavity produces considerable overlap of the pulses such that the temporal intensity profile may be considered to be a prolonged single pulse with a modification to the falling edge of the intensity profile and it is possible that the spectral feature can be attributed to this form of pulse shaping influencing the evolution of the TNSA mechanism. A similar feature was also observed by Markey *et al.*[11] where the rising edge of a 0.7 ps pulse is shaped by the introduction of a prepulse and have a similar intensity ratio to that here at 0.4:1. The multi-pulse sheath acceleration mechanism[10] is predicted to produce spectral peaks and may be responsible for the presence of this feature.

The exact spectral shape of the high dose feature remains in question as the RCF detector does not have the

resolution required to differentiate between the presence of a low energy peak or a flattening of the spectrum. With many applications demanding spectral peaks and where flatter proton spectra provide a means for uniform isochoric heating, especially where the uniformity of proton heating has been a challenge until present, investigation into the mechanism producing this feature is warranted and a Thomson parabola ion spectrometer[20] which has high spectral resolution at low energy will be fielded on future experiments.

While thick targets were used in this study to investigate the principle of the target design, thin targets will be used to investigate further conversion efficiency enhancement[21] in conjunction with plasma mirrors.

The authors gratefully acknowledge the expert assistance of both the Target Fabrication group of the Central Laser Facility and the PHELIX operations team and funding from EPSRC (Grant Nos. EP/E048668/1 and EP/E035728/1) and the European Community's Seventh Framework Programme (Grant No. 228334).

[1]S. C. Wilks, A. B. Langdon, T. E. Cowan, M. Roth, M. Singh, S. Hatchett, M. H. Key, D. Pennington, A. MacKinnon, and R. A. Snavely, Phys. Plasmas **8**, 542 (2001).
[2]S. V. Bulanov, T. Zh Esirkepov, V. S. Khoroshkov, A. V. Kuznetsov, and F. Pegoraro, Phys. Lett. A **299**, 240 (2002).
[3]P. K. Patel, A. J. MacKinnon, M. H. Key, T. E. Cowan, M. E. Foord, M. Allen, D. F. Price, H. Ruhl, P. T. Springer, and R. Stephens, Phys. Rev. Lett. **91**, 125004 (2003).
[4]M. Temporal, J. J. Honrubia, and S. Atzeni, Phys. Plasmas **9**, 3098 (2002).
[5]M. Roth, T. E. Cowan, M. H. Key, S. P. Hatchett, C. Brown, W. Fountain, J. Johnson, D. M. Pennington, R. A. Snavely, S. C. Wilks *et al.*, Phys. Rev. Lett. **86**, 436 (2001).
[6]Y. Ping, R. Shepherd, B. F. Lasinski, M. Tabak, H. Chen, H. K. Chung, K. B. Fournier, S. B. Hansen, A. Kemp, D. A. Liedahl *et al.*, Phys. Rev. Lett. **100**, 085004 (2008).
[7]M. J. V. Streeter, P. S. Foster, F. H. Cameron, M. Borghesi, C. Brenner, D. C. Carroll, E. Divall, N. P. Dover, B. Dromey, P. Gallegos *et al.*, New J. Phys. **13**, 023041 (2011).
[8]M. Nakatsutsumi, A. Kon, S. Buffechoux, P. Audebert, J. Fuchs, and R. Kodama, Opt. Lett. **35**, 2314 (2010).
[9]J. Badziak, S. Borodziuk, T. Pisarczyk, T. Chodukowski, E. Krousky, K. Masek, J. Skala, J. Ullschmied, and Y.-J. Rhee, Appl. Phys. Lett. **96**, 251502 (2010).
[10]A. P. L. Robinson, D. Neely, P. McKenna, and R. G. Evans, Plasma Phys. Controlled Fusion **49**, 373 (2007).
[11]K. Markey, P. McKenna, C. M. Brenner, D. C. Carroll, M. M. Günther, K. Harres, S. Kar, K. Lancaster, F. Nürnberg, M. N. Quinn *et al.*, Phys. Rev. Lett. **105**, 195008 (2010).
[12]O. Lundh, F. Lindau, A. Persson, C.-G. Wahlström, P. McKenna, and D. Batani, Phys. Rev. E **76**, 026404 (2007).
[13]J. Fuchs, P. Antici, E. D'Humières, E. Lefebvre, M. Borghesi, E. Brambrink, C. A. Cecchetti, M. Kaluza, V. Malka, M. Manclossi *et al.*, Nat. Phys. **2**, 48 (2005).
[14]P. Mora, Phys. Rev. Lett. **90**, 185002 (2003).
[15]L. Robson, P. T. Simpson, R. J. Clarke, K. W. D. Ledingham, F. Lindau, O. Lundh, T. McCanny, P. Mora, D. Neely, C.-G. Wahlström, M. Zepf, and P. McKenna, Nat. Phys. **3**, 58 (2007).
[16]P. McKenna, D. C. Carroll, O. Lundh, F. Nürnberg, K. Markey, S. Bandyopadhyay, D. Batani, R. G. Evans, R. Jafer, S. Kar *et al.*, Laser Part. Beams **26**, 591 (2008).
[17]Y. Sentoku, V. Y. Bychenkov, K. Flippo, A. Maksimchuk, K. Mima, G. Mourou, Z. M. Sheng, and D. Umstadter, Appl. Phys. B **74**, 207 (2002).
[18]T. Grismayer and P. Mora, Phys. Plasmas **13**, 032103 (2006).
[19]J. Fuchs, C. A. Cecchetti, M. Borghesi, T. Grismayer, E. D'Humières, P. Antici, S. Atzeni, P. Mora, A. Pipahl, L. Romagnani *et al.*, Phys. Rev. Lett. **99**, 015002 (2007).
[20]D. C. Carroll, P. Brummitt, D. Neely, F. Lindau, O. Lundh, C.-G. Wahlström, and P. McKenna, Nucl. Instrum. Methods A **620**, 23 (2010).
[21]D. Neely, P. Foster, A. Robinson, F. Lindau, O. Lundh, A. Persson, C.-G. Wahlström, and P. McKenna, Appl. Phys. Lett. **89**, 021502 (2006).